

Article

Multi-Objective Structural Optimization Design for Electric Excavator-Specific Battery Packs with Impact Resistance and Fatigue Endurance

Zihang Li ¹, Jiao Qin ¹, Ming Zhao ², Minmin Xu ¹ , Wei Huang ¹ and Fangming Wu ^{2,*}

¹ School of Mechanical Engineering, Guangxi University, Nanning 530004, China; 2211392009@gxu.edu.cn (Z.L.); 2311391110@gxu.edu.cn (J.Q.); mmmxu@gxu.edu.cn (M.X.); huangwei@gxu.edu.cn (W.H.)

² Guangxi Liugong Machinery Co., Ltd., Liuzhou 545007, China; zhaom@liugong.com

* Correspondence: wufangming@liugong.com

Abstract: As the issue of energy scarcity becomes increasingly critical, the adoption of electric construction machinery emerges as a pivotal strategy to address the energy crisis. During the travel and operation of electric construction machinery, the machinery-specific battery packs are subjected to long-term mechanical shocks and random vibration loads, leading to resonance and structural damage failure. To address the multi-objective optimization design issues of machinery-specific battery packs for electric construction machinery under the action of random vibration and impact loads and to enhance the fatigue life and reduce the mass of the battery pack, this paper conducts optimization design research on a newly developed battery pack for an electric excavator. Firstly, a finite element model of the battery pack is established to conduct simulation analyses on its impact resistance characteristics and fatigue life. Secondly, through a comprehensive contribution analysis method, key components are identified, with the thickness dimensions of the battery pack parts selected as design parameters. Finally, using maximum stress under mechanical shock conditions and first-order constraint mode as constraint conditions, mass minimization and fatigue life maximization are set as optimization objectives. The Box–Behnken experimental design is employed alongside a Kriging approximation model; subsequently, the NSGA-II algorithm is utilized for multi-objective optimization. The optimization results show that, while meeting the basic static and dynamic performance requirements, the mass of the optimized battery pack outer frame is reduced by 56.8 kg, a decrease of 5.75%. Concurrently, the optimized battery pack's fatigue life has increased by 1,234,800 cycles, which is an enhancement factor of 1.65 compared to pre-optimization levels. These findings provide significant reference points for optimizing structural performance and achieving lightweight designs in electric excavator battery packs.

Keywords: battery pack; mechanical impact; fatigue life; multi-objective optimization; lightweight design



Academic Editor: JongHoon Kim

Received: 31 December 2024

Revised: 24 January 2025

Accepted: 28 January 2025

Published: 31 January 2025

Citation: Li, Z.; Qin, J.; Zhao, M.; Xu, M.; Huang, W.; Wu, F. Multi-Objective Structural Optimization Design for Electric Excavator-Specific Battery Packs with Impact Resistance and Fatigue Endurance. *Energies* **2025**, *18*, 669. <https://doi.org/10.3390/en18030669>

Copyright: © 2025 by the authors. Licensee MDPI, Basel, Switzerland. This article is an open access article distributed under the terms and conditions of the Creative Commons Attribution (CC BY) license (<https://creativecommons.org/licenses/by/4.0/>).

1. Introduction

With the advancement of battery technology and the increasing environmental protection requirements imposed by various countries, electric construction machinery has begun to see widespread application across diverse settings [1–3]. Currently, electric technology is extensively employed in the automotive sector. However, excavators exhibit significant structural differences and distinct operating conditions compared to automobiles, which

complicates the direct adaptation of electric vehicle technology for use in electric excavators. There are fundamental disparities between excavators and automobiles regarding transmission methods, working characteristics, and operational environments [4,5]. The operating conditions of electric excavators are complex, with drastic power fluctuations and high power density demands, which require a larger battery capacity; this results in a heavier battery pack and a higher center of gravity [6–8].

In past incidents involving battery pack safety, many accidents were attributed to insufficient mechanical reliability of the battery packs [9]. The vibrations generated during the operation of electric engineering machinery can adversely affect the lifespan of these battery packs and lead to structural fatigue failures [10]. Electric excavators, in particular, produce intense vibrations while working, especially during demolition tasks, subjecting the entire machine body to prolonged random vibrations. When battery packs are subjected to such random vibrational loads over extended periods, their failure rate can reach as high as 20%. This condition increases the likelihood of weld seam cracking, which may result in circuit interruptions and misalignment within the battery pack [11]. To address the impacts of random vibrations, numerous scholars from various countries have conducted extensive research on battery packs. Hye-gyu K et al. proposed a structural design for battery packs utilizing multiple materials and evaluated its performance through random vibration fatigue tests. The experimental results demonstrated that the fatigue life of the multi-material battery pack meets requirements while also reducing the overall weight of the pack [12]. Li Shui et al. employed a combination of four optimization methods to establish models for maximum deformation, minimum natural frequency, and mass of the battery pack. They designed experiments based on optimal combinations and ultimately derived an optimal solution using the NSGA-II algorithm for manufacturing the battery pack casing [13]. Pan YJ et al. developed a nonlinear dynamic finite element model for battery packs and performed extrusion and collision simulations with this model. By employing various high-strength materials in lightweight design strategies, they successfully reduced the mass of the battery pack while enhancing its impact resistance [14]. Zhang XX et al. established a nonlinear finite element model of the battery system and conducted crush and random vibration simulations to obtain the crush stress and fatigue life, subsequently developing a third-order response surface model to elucidate the relationship between component thickness, compressive stress, and fatigue life. Finally, they formulated an optimization model aimed at maximizing the fatigue life of the battery system while ensuring that the compressive stress does not exceed permissible limits [15]. Due to harsh working environments, specialized battery packs for excavators are susceptible to severe impacts from various unexpected conditions; for instance, when an electric excavator falls from a height, its battery pack can easily suffer from significant shocks leading to weld seam fractures and connection failures. When the battery pack is subjected to excessive impact stress, it has a higher failure rate, with the positive and negative terminals of the battery pack being susceptible to fracture, leading to reduced capacity and power; moreover, excessive stress can damage the battery pack casing, resulting in short circuits. To address the mechanical impact loads experienced by battery packs, PAN YJ et al. enhanced their strength through high-strength steel usage combined with dimensional optimization strategies. This approach successfully met the requirements for preventing damage under mechanical shock conditions while achieving a 10.41% reduction in the weight of the optimized battery pack [16]. When battery packs are subjected to random vibrations over the long-term, affecting their fatigue life, structural design can be integrated with the actual operating conditions of the battery pack, and finite element analysis under vibration conditions can be performed to improve the fatigue life, ensuring the safety of the battery pack in a vibrating environment [17]. The aforementioned studies focused on

structural dimension design, modal analysis, fatigue life assessment, and mechanical shock analysis of battery packs individually while conducting certain optimizations related to mass reduction and fatigue lifespan enhancement. However, most battery pack research is confined to the field of electric vehicles, with little research conducted on battery packs specifically for electric construction machinery. Moreover, the focus has predominantly been on light-weighting initiatives without considering multiple parameters such as modal characteristics, stress during impact scenarios, and overall fatigue lifespan concurrently, thus lacking comprehensive approaches towards optimizing both durability against wear over time as well as minimizing weight effectively.

In summary, the majority of current simulation experiments for battery packs focus on verifying the structural strength and fatigue life of battery packs for electric vehicles, optimizing for a single objective. There is a lack of multi-objective optimization designs for battery packs under various operating conditions. Moreover, most research is conducted on battery packs for electric vehicles, with relatively little attention given to those for construction machinery. There is a need for analysis and optimization of battery packs specifically for the unique operating conditions of construction machinery. To address these issues, it is of great significance to conduct mechanical impact simulations and random vibration fatigue analyses of battery packs based on the actual usage environment of excavators. This ensures that the battery packs meet design strength requirements and provides a basis for predicting fatigue life and lightweight design of the battery packs. The present study focuses on the battery pack of a newly developed 22-ton electric excavator by a specific enterprise. Based on the Chinese standard GB/T 44257.1-2024, titled "Traction battery of electric earth-moving machinery-Part 1: Safety requirements," a simulation analysis of the battery pack is conducted. The optimization objectives are to reduce the mass of the battery pack and to enhance its fatigue life. By integrating the Kriging approximation model with the second-generation non-dominated sorting genetic algorithm (NSGA-II), a multi-objective optimization design is conducted. This approach offers a strategy for the optimized design of battery packs specifically for electric construction machinery.

2. Establishment of Finite Element Model for Electric Excavator Battery Pack

The battery pack of a specific electric excavator is designed with a three-layer cell structure to meet the demands for high power and large capacity. The battery pack primarily consists of the battery module and an outer frame, with a total weight of 3747 kg. The battery module is composed of a liquid cooling plate, end plates, and 38 individual cells. The material used for the liquid cooling plate is 3003-H18, which is located at the bottom of the individual cells to facilitate heat dissipation; the end plates are made from 3004-H38 and are positioned on the sides of the individual cells to secure them in place. The outer frame of the battery pack comprises covering components and a frame. The frame is constructed from Q345 steel, serving as the main load-bearing component; it connects to the vehicle chassis through mounting holes located at its base. The covering components are made from Q235 steel, primarily functioning to provide sealing and ensure airtightness within the battery pack. To reduce production costs for the battery pack, it is required that no alterations be made to its component shapes during optimization processes. Additionally, given that the specifications for securing bolts in the battery module are M8, the thickness of the battery pack's framework must not fall below 16 mm to maintain airtight integrity. The basic parameters for these materials can be found in Table 1.

Table 1. Properties of battery pack materials.

Material Name	Elastic Modulus/(MPa)	Poisson's Ratio	Yield Strength/(MPa)	Density/(kg·m ⁻³)
3003-H18	68,948	0.33	181	2740
3004-H38	68,948	0.33	240	2740
Q235	210,000	0.274	235	7830
Q345	210,000	0.31	345	7870

The finite element model was established by extracting the mid-surface of the battery pack's outer frame, utilizing 8 mm shell elements for mesh generation. The batteries within the battery module are treated with homogenization and meshed using hexahedral elements. The weld seams of the battery pack's outer frame are simulated using seam elements, and bolted connections are represented by rigid elements that connect the nodal points at the edges of the bolt holes. The total number of elements in the finite element model is 1,849,467, and the total number of nodes is 2,193,746. The Jacobian ratio is not lower than 0.7, ensuring the quality of the mesh. To improve the efficiency of the simulation, the finite element model is simplified by neglecting components that are not crucial for the simulation analysis, such as busbars, electrical components, and pipes. The battery pack model is shown in Figure 1.

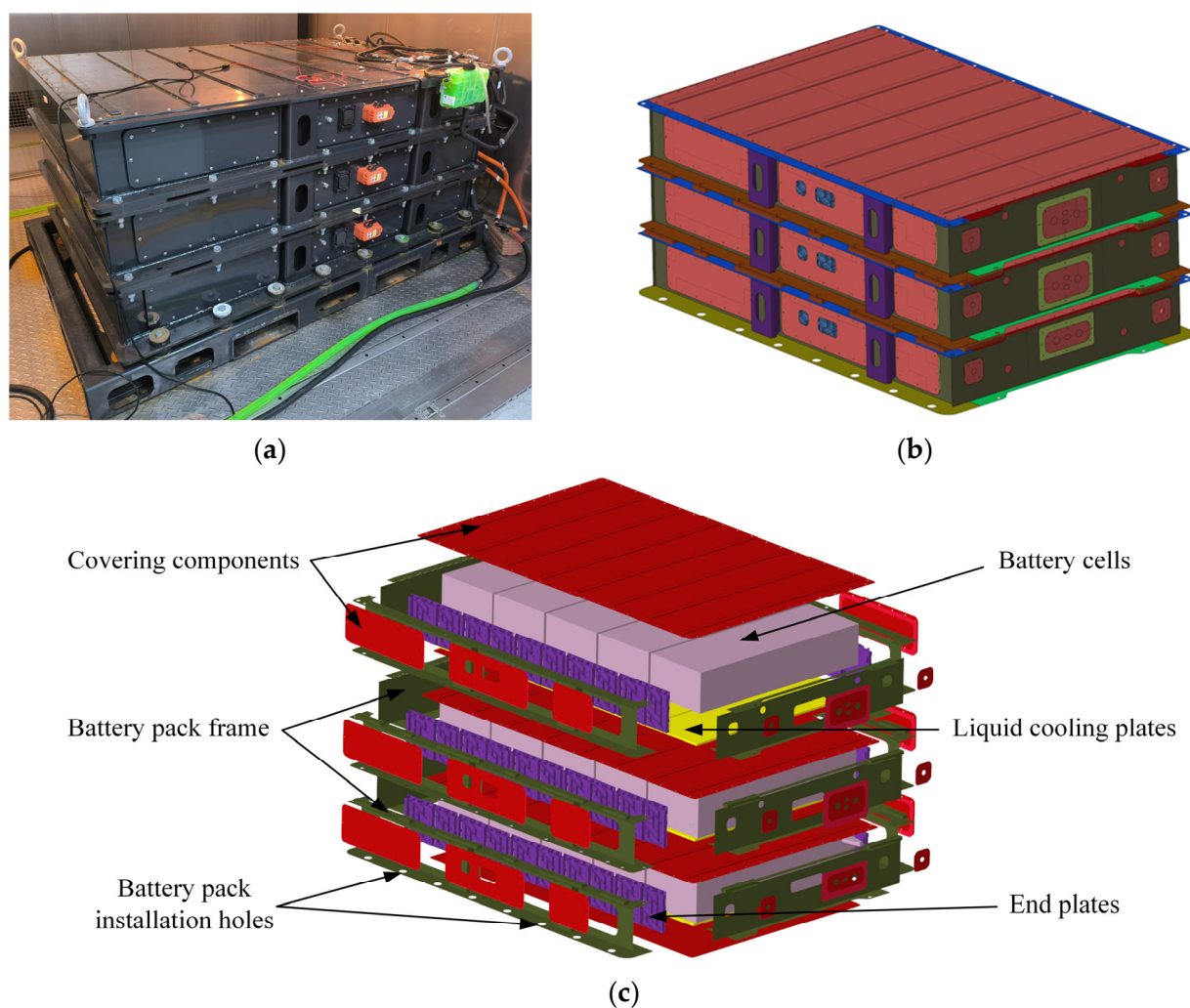


Figure 1. Image of the battery pack: (a) Physical image of the battery pack; (b) Finite element model diagram of the battery pack; (c) Battery pack structure diagram.

As shown in Figure 1, the battery pack of the electric excavator is divided into three layers, with each layer containing five battery modules. The outer frame of the battery pack can also be divided into a similar three-layer structure, consisting of covering components and a supporting framework.

3. Battery Pack Structural Simulation Analysis

3.1. Modal Analysis of Battery Pack Constraints

To prevent resonance of the battery pack during the operation and movement of the electric excavator, it is essential to determine the natural frequency of the battery pack under actual working conditions and to understand its dynamic characteristics. Based on the installation requirements of the battery pack on the electric excavator, a constrained modal analysis was conducted using a finite element model [18]. Based on the actual connection relationship between the battery pack and the excavator, boundary conditions were established to constrain all degrees of freedom of the 16 installation holes of the battery pack shown in Figure 1c. A constrained modal simulation was then carried out to extract the first six natural mode frequencies and their corresponding mode shapes, as shown in Figure 2.

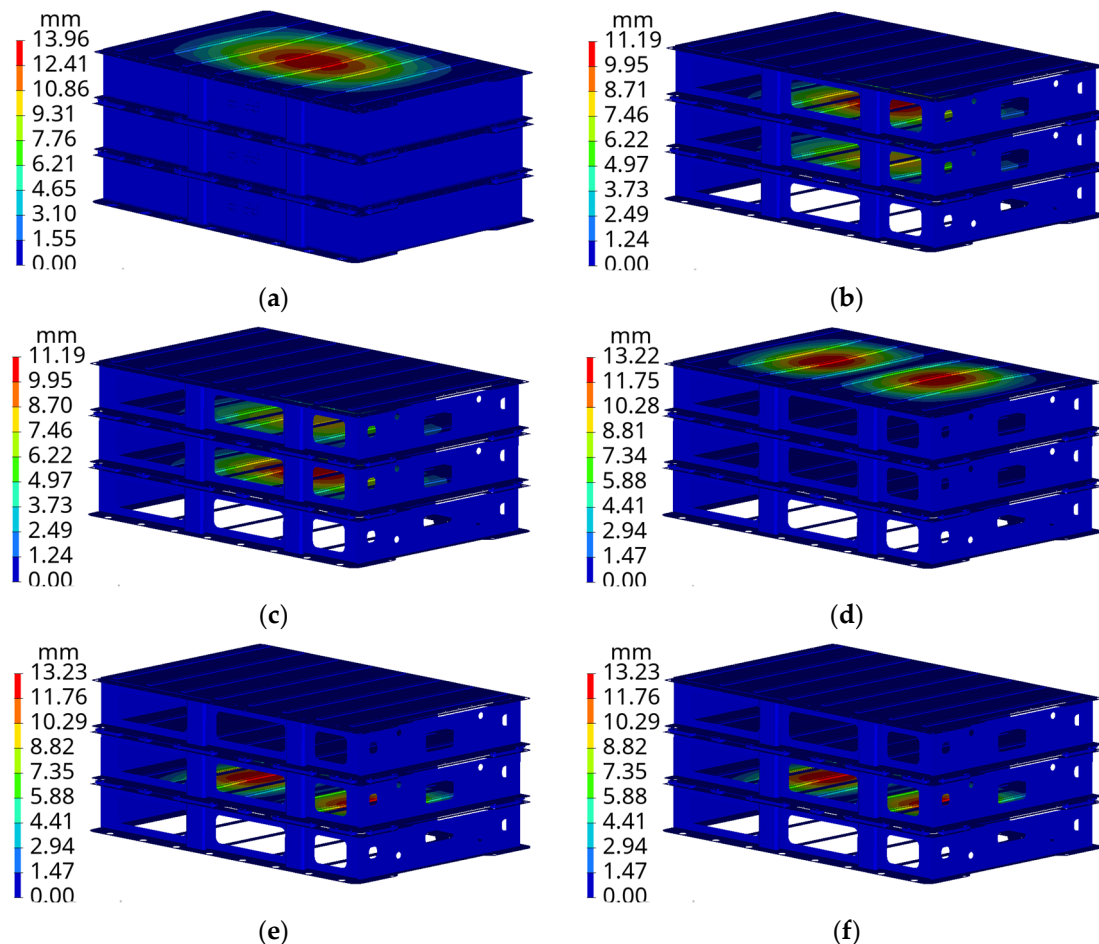


Figure 2. Modal diagram of the battery pack: (a) First-order modalities; (b) Second-order modes; (c) Third-order modalities; (d) Fourth-order modes; (e) Fifth-order modalities; (f) Sixth-order modes.

In Figure 2, the first-order modal resonance regions are distributed at the center of the top cover of the battery pack box, vibrating up and down along the Z direction; the second- and third-order modal resonance regions are distributed at the center of the middle and bottom layers of the battery pack box, respectively, with similar modes as the first-order

modal. The fourth-order modal resonance region is distributed at the center of the top cover of the battery pack box, with two symmetrical resonance regions along the Z direction vibrating up and down alternately with opposite directions; the fifth- and sixth-order modal resonance regions are distributed at the center of the bottom and middle layers of the battery pack box, respectively, with similar modes as the fourth-order modal. The first six order modal resonance regions of the battery pack are mainly distributed at the top cover of each layer of the battery pack, mainly vibrating up and down along the Z direction, with specific natural frequencies listed in Table 2. The external excitations acting on electric excavator battery packs primarily originate from road surfaces as well as hydraulic pumps and motors, but the excitation generated by the hydraulic pump and motor is attenuated by damping pads and mounting brackets, so it can be ignored when transferred to the battery pack, therefore mainly considering the vibration from the ground. The excitations experienced by the components of electric excavators primarily originate from the road surface during movement as well as from the vibrations generated by the operation of hydraulic pumps and motors. However, unlike traditional excavators, in electric excavators, the hydraulic pump and motor are not directly connected to the battery pack. Instead, they are linked to the chassis through mounting brackets and shock absorbers. Similarly, the battery pack is connected to the chassis via a quick-change frame and shock absorbers. The excitations generated by the hydraulic pump and motor when operating can be neglected after attenuation by the mounting brackets, shock absorbers, chassis, quick-change frame, and shock absorbers before being transferred to the battery pack. In addition, the excitation generated by the hydraulic pumps and motors has a more defined periodicity, which is weakly randomized compared to the excitation from the road surface. Therefore, the excitations to the battery pack mainly come from the road surface excitation when the electric excavator is traveling. During operation, a tracked excavator experiences ground excitation of approximately 10 Hz [19], so the battery pack will not resonate due to road excitation. Considering that the first-order natural frequency of the battery pack is likely to coincide with ground excitation during optimization and cause resonance, the first-order natural mode of the battery pack is set as the structural response Q as the subsequent structural optimization response variable.

Table 2. Constrained modal frequencies of the battery.

Modal Order	First-Order Modalities	Second-Order Modes	Third-Order Modalities	Fourth-Order Modes	Fifth-Order Modalities	Sixth-Order Modes
Frequency (Hz)	21.50	21.59	21.60	23.17	23.23	23.24

3.2. Simulation Analysis of Mechanical Impact on Battery Packs

In order to evaluate the ability of the battery pack to resist deformation and damage under mechanical impact conditions, a simulation analysis of mechanical impact on the battery pack was conducted. Firstly, an RBE2 element was rigidly connected to 16 installation holes of the battery pack shown in Figure 1c, and a node was generated at the center of the bottom of the battery pack. All degrees of freedom of this node are then constrained, and mechanical impact loads in the $\pm Z$ direction are applied at the node according to the national standards of China. The maximum stress obtained from the simulation is compared to the allowable stress of the battery pack material to determine whether damage will occur after the mechanical impact. The load curve applied during the mechanical impact simulation experiment is illustrated in Figure 3.

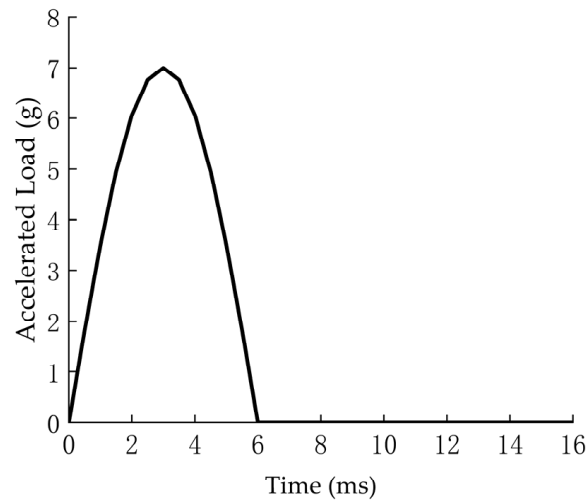


Figure 3. Load curve graph.

In Figure 3, in accordance with the national standards of China, a half-sine shock wave with a peak value of 7 g and a duration of 6 ms is applied to the battery pack. The time interval between two consecutive shocks is determined based on ensuring that their responses do not interfere with each other on the test sample [20]. Therefore, during the simulation, separate experiments are conducted for the $\pm Z$ direction of the battery pack. The peak acceleration is set at 7 g, with a total simulation duration of 15 ms; loads are applied for the first 6 ms, followed by a 9 ms observation period to assess the stress conditions experienced by the battery pack. The simulation results are presented in Figure 4.

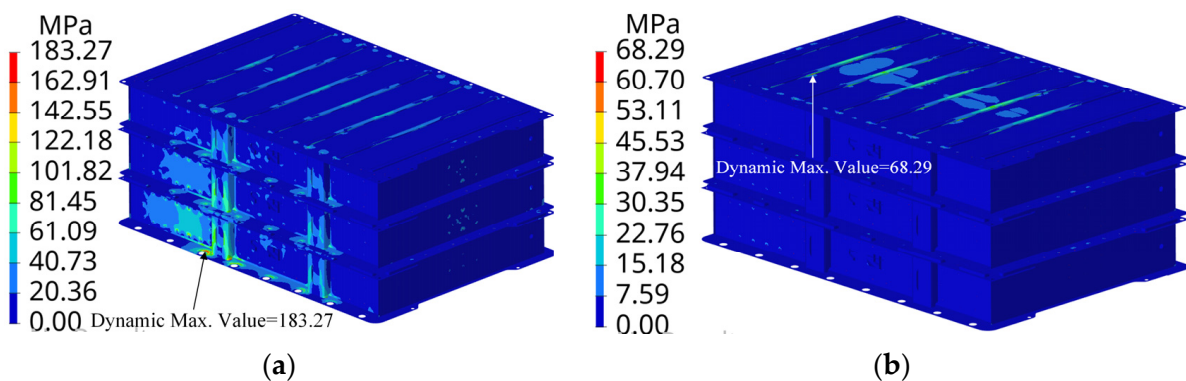


Figure 4. Stress contour map under mechanical impact conditions: (a) +Z direction operating condition; (b) $-Z$ direction operating condition.

In Figure 4, when a mechanical impact is applied to the battery pack in the +Z direction, the maximum impact stress S_1 occurs at the center mounting hole of the bottom mounting plate, with a magnitude of 183.3 MPa, which is below the yield strength of material Q345. When a mechanical impact is applied in the $-Z$ direction, the maximum impact stress S_2 appears at the location of the cover plate reinforcement ribs, measuring 68.29 MPa and remaining below the allowable stress for this material. Based on the simulation experiment results of mechanical impact, the strength of the battery pack components meets the requirements, and the maximum impact stresses S_1 and S_2 in both $\pm Z$ directions are set as the structural performance response to be used as the response variable for subsequent experimental design and optimization models.

3.3. Simulation Analysis of Battery Pack Fatigue Life

The present study employs the frequency domain method to predict the fatigue life of battery packs. Initially, a frequency response analysis is conducted on the battery pack to obtain its response function under unit excitation, followed by the generation of finite element results. Subsequently, the finite element results obtained from the frequency response analysis are combined with the ZYX direction power spectral density required by the national standards of China, and the material correction to the S-N curve is used to predict the fatigue life of the battery pack.

3.3.1. Frequency Response Analysis of Battery Packs

Frequency response analysis is mainly used to calculate the dynamic response of the structure to different frequencies under unit excitation. By performing Fourier transformation on the excitation and output responses, the frequency response function can be obtained. Based on the actual installation conditions of the electric excavator's battery pack, boundary conditions are established by constraining all degrees of freedom at the bottom mounting holes of the battery pack. A unit acceleration load ($g = 9800 \text{ mm/s}^2$) is applied in the ZYX directions, with a structural damping ratio selected as 0.05 [21]. The stress response curve of the battery pack under unit excitation can be determined based on the frequency response analysis results. For instance, the Z-axis stress response under unit excitation is shown in Figure 5, and it is observed that maximum stress occurs around 21 Hz, which aligns with the first-order modal frequency of the battery pack.

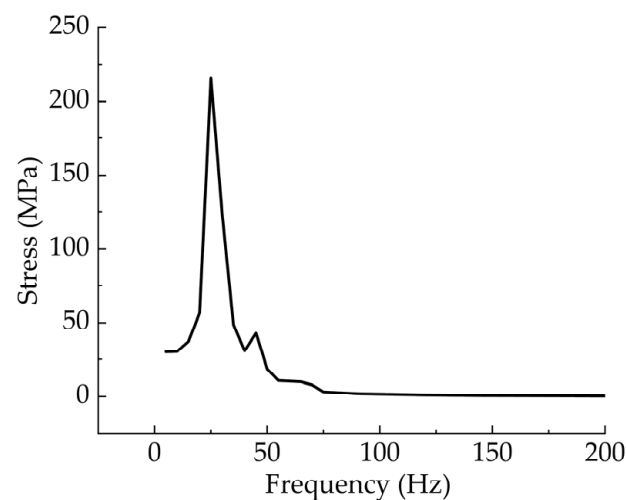


Figure 5. Frequency response diagram.

3.3.2. Prediction of Battery Pack Fatigue Life

In the nCode software (nCode2020R2), a random vibration fatigue life analysis process is established. The results of frequency response analysis, PSD spectrum, and the life analysis module are interconnected. Additionally, material-corrected S-N curves are utilized to apply cyclic loads. Using Miner's linear damage theory, the damage incurred by each cycle of loading on the battery pack structure is aggregated. The Goodman method is employed to adjust for the impact of mean stress on fatigue life, with a model survival rate set at 50%. The PSD cycle counting method applied is Dirlik's approach. The fatigue life cloud map of the electric excavator battery pack has been calculated, as illustrated in Figure 6.

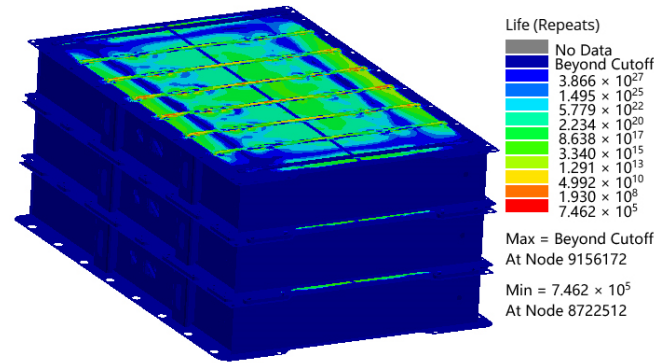


Figure 6. Fatigue life contour map.

The national standards of China require that the fatigue acceleration testing time for battery packs be no less than 21 h. In this context, one second represents a single cycle, which translates to a minimum cycle life of 75,600 cycles [22]. As illustrated in Figure 6, the lowest fatigue life of the battery pack occurs at the reinforcement ribs of the upper cover plate, with a minimum cycle count of 746,200 cycles. This indicates that the accelerated fatigue life of the battery pack is approximately 207.28 h; thus, it meets the national standard requirement of 21 h. The primary resonance region of the battery pack is concentrated around its upper cover. According to the frequency response graph presented in Figure 5, when subjected to random vibration loads, the stress at the top cover of the battery pack is the highest, leading to the greatest damage and lowest fatigue life. To enhance the fatigue life of the battery pack in electric excavators, the minimum cycle life of the battery pack is established as structural response L. This will serve as a performance indicator for the subsequent multi-objective optimization of the battery pack.

4. Battery Pack Multi-Objective Optimization Design

4.1. Selection of Variables for Multi-Objective Optimization in Battery Packs

To achieve a lightweight design for the battery pack that is resistant to impact and fatigue while maintaining the spatial structure and component shapes, this study employs the thickness of battery pack components as a design parameter for multi-objective optimization. Given the multitude of parts in the battery pack and the interdependent nature of some parameters, it is necessary to identify parameters that significantly influence the mass of the battery pack and its structural response under various operating conditions. This paper employs the comprehensive contribution analysis (CCA) method to screen the parameters of the battery pack components. The CCA allows for identifying critical design parameters from complex structures with many parts by highlighting those that have a substantial effect on response variables while eliminating less impactful ones. In this approach, the model's response variable can be approximated through a multiple regression model based on design parameters [23]:

$$Y(x_1, x_2, \dots, x_n) = \alpha + \sum_i^N H_i(x_i) + \sum_{i=2}^N \sum_{j=1}^{i-1} R_{ij}(x_i, x_j) + \beta \quad (1)$$

In the equation, Y represents the structural response variable of the model; x_i denotes the design parameters of the model; α is a constant; N indicates the number of design parameters in the model; $H_i(x_i)$ signifies the main effects of design parameters; $R_{ij}(x_i, x_j)$

refers to the interaction effects between any two design parameters; and β represents error values. The main effect of each design parameter can be expressed as follows:

$$\sum_{i=1}^N H_i(x_i) = \sum_{i=1}^N \lambda_i x_i \quad (2)$$

Here, λ_i stands for the coefficient of main effects for design parameters, thus indicating that the contribution degree of a specific design parameter to structural response is given by the following:

$$e_i = \frac{100\lambda_i}{\sum_{i=1}^N |\lambda_i|} \quad (3)$$

Consequently, the comprehensive contribution degree of a design parameter to structural responses can be represented as follows:

$$E_i = \frac{1}{N} \sum_{j=1}^N e_j \quad (4)$$

Here, E_i is the comprehensive contribution degree of a single design parameter to multiple structural responses. The components within the battery pack that possess identical shapes and thicknesses are categorized into a single group. Considering the structural responses and mass response M of the battery pack, 10 sets of components were selected from the battery pack for a comprehensive contribution analysis. According to the processing technology and the requirements for bolt length, the upper and lower limits of dimensions for 10 sets of components were determined. A fractional factorial design with 10 factors at two levels is employed to create an experimental plan, resulting in 24 sets of experimental size data. Simulation analysis and extraction of simulation results are performed according to experimental groups. In HyperStudy software (HyperStudy2020), input the dimensional parameters of each experimental group and the corresponding simulation results, and the software will calculate the impact of the change in each dimensional parameter of each part on the simulation results according to Equations (1)–(4), i.e., the contribution degree. The contribution of each size parameter to different simulation conditions can be summed up and divided by the number of simulation conditions to obtain the comprehensive contribution. The results are shown in Figure 7.

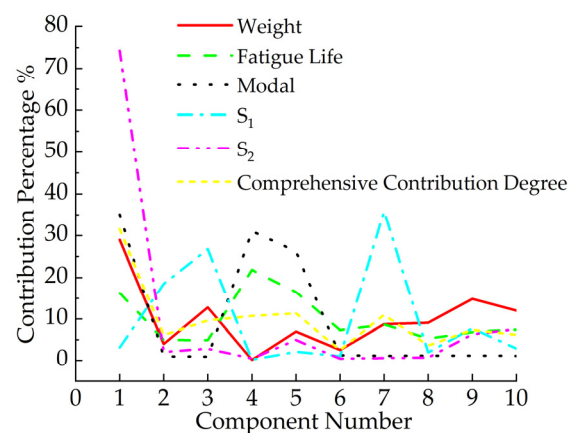


Figure 7. Comprehensive contribution chart for components.

In Figure 7, based on the results of the comprehensive contribution analysis, the top seven part sizes that have a significant impact on the various responses can be selected as

design parameters for the multi-objective optimization of the battery pack. The components are sequentially designated as t_i , where i represents the component number.

4.2. Box–Behnken Experimental Design

Adopting a rational experimental design scheme is conducive to generating appropriate experimental groups, thereby enhancing the efficiency of the experiment and reducing experimental errors. The Box–Behnken design is a three-level fractional factorial experiment method that fits a quadratic polynomial based on the method of least squares to determine the coefficients of the quadratic terms. This experimental approach can uniformly cover the design space, assess the non-linear effects of factors, and minimize experimental errors [24,25]. According to the results of the simulation experiments and the fatigue endurance and lightweight requirements of the battery pack, the fatigue life L and mass M of the battery pack are taken as optimization objectives; the first-order mode Q of the battery pack and the maximum stress S_1, S_2 under $\pm Z$ -direction mechanical impact are considered as constraints. The upper and lower limits of the seven groups of part sizes filtered through the comprehensive contribution analysis are determined. Utilizing the Box–Behnken experimental design methodology, 57 sample points were automatically generated. The experiments were conducted according to the design parameters of each group of sample points, and the results are extracted, including the first-order mode Q of the battery pack; fatigue life L ; mass M ; and the maximum impact stress S_1, S_2 in the $\pm Z$ direction.

4.3. Establishment of Approximate Models and Error Verification

The Kriging method establishes an approximation model by combining a global surrogate model with local deviations, thereby elucidating the relationship between design parameters and responses. This method demonstrates superior fitting performance for high-order nonlinear problems. The Kriging approximation model can be expressed as follows [26,27]:

$$f(x) = h(x) + z(x) \quad (5)$$

In this expression, $f(x)$ represents the target function to be fitted; $h(x)$ denotes the polynomial approximation model, generally being a constant; $z(x)$ is a random deviation with a variance of σ^2 , an expectation of zero, and a non-zero covariance. This characteristic allows for the Kriging model to perform interpolation between sample points, which is why it is also referred to as a spatial local interpolation method. To assess the reliability of the Kriging model, one can evaluate its fitting accuracy using the coefficient of determination R^2 . The value of R^2 ranges from 0 to 1; values closer to 1 indicate higher fitting precision. The expression for R^2 is given by the following [28]:

$$R^2 = \frac{\sum_{i=1}^N (\hat{y}_i - \bar{y})}{\sum_{i=1}^N (y_i - \bar{y})} \quad (6)$$

In the equation, \hat{y}_i represents the predicted response value at the i -th point; y_i denotes the actual response value at the i -th point; and \bar{y} signifies the average response value. Twenty sample points are randomly selected, and based on the predicted values of the structural response from the Kriging model and the simulation values, the R^2 values for the mass response M , fatigue life response L , first-order mode response Q , maximum stress response in the $+Z$ direction S_1 , and maximum stress response in the $-Z$ direction S_2 are obtained, as shown in Figure 8.

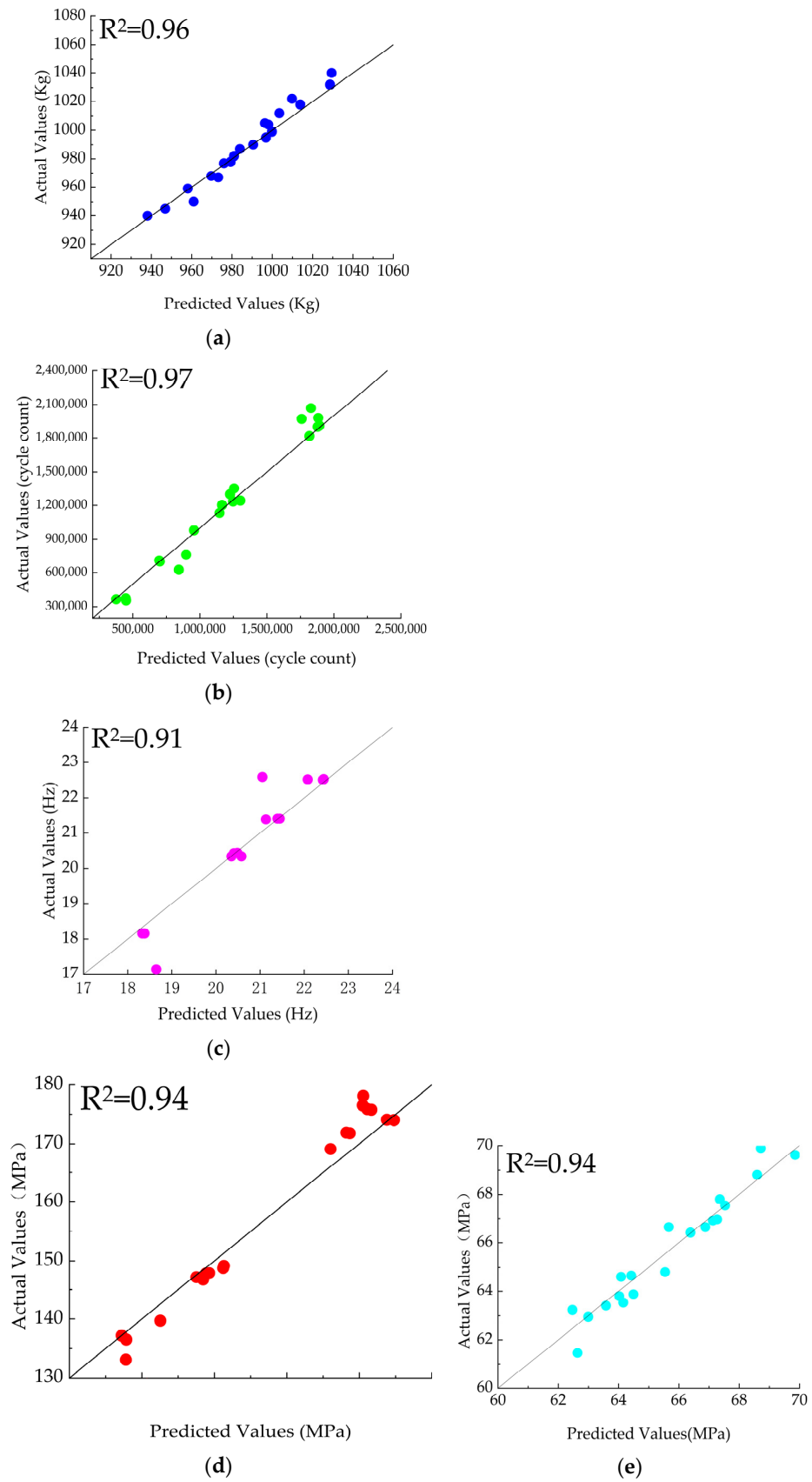


Figure 8. Structural response R^2 graph: (a) Mass R^2 chart; (b) Fatigue life R^2 chart; (c) First-order mode R^2 chart; (d) Maximum stress in the +Z direction R^2 chart; (e) Maximum stress in the -Z direction R^2 chart.

In Figure 8, the correlation coefficients R^2 for the mass response M and fatigue life response L are 0.96 and 0.97, respectively. The R^2 values for the modal response Q , maximum impact stress responses in both $\pm Z$ directions S_1 and S_2 are 0.91, 0.94, and 0.94, respectively; all of which exceed 0.9. This indicates that the established Kriging approximation model demonstrates good accuracy and reliability.

4.4. Establishment and Solution of the Optimization Model

To ensure the safety and reliability of the battery pack, it is typically designed with a performance margin, indicating room for optimization. By employing appropriate optimization methods, it is possible to effectively reduce computational costs while obtaining a sufficient number of uniformly distributed and convergent Pareto optimal solutions. The NSGA-II combined with an elitism strategy use crowding distance and crowding distance comparison operators to enhance computational efficiency and optimization accuracy. This ensures that the optimal front solutions are uniformly distributed across the Pareto domain, and the method is robust with strong exploration capabilities. In order to achieve multi-objective optimization of the battery pack, the NSGA-II algorithm is utilized, with the objectives of minimizing the mass M of the battery pack and maximizing its fatigue life L . The constraints for the optimization include the first-order mode Q and the maximum impact stress responses in the $\pm Z$ direction S_1 and S_2 . The optimization model is as follows:

$$\left\{ \begin{array}{l} \text{find } T = (t_1, t_2, \dots, t_6, t_7) \\ \text{min } M, -L \\ \text{s.t. } \left\{ \begin{array}{l} 10 \text{ Hz} \leq Q \\ S_1 \leq 345 \text{ MPa} \\ S_2 \leq 235 \text{ MPa} \\ t_i [t_{i\text{min}}, t_{i\text{max}}], i = 1, 2, \dots, 6, 7 \end{array} \right. \end{array} \right. \quad (7)$$

The population size is set to 20, and the number of generations is set to 100 to obtain the Pareto optimal solution set for multi-objective optimization, as shown in Figure 9.

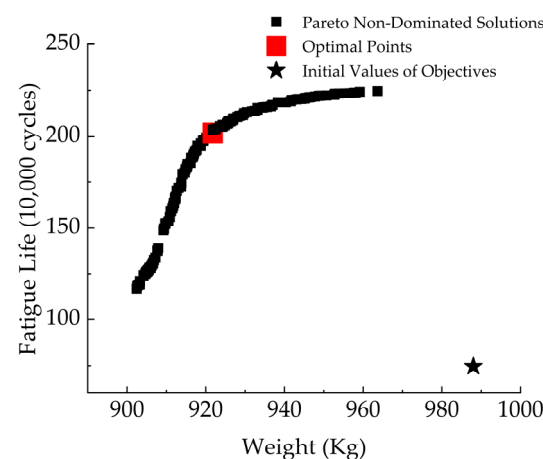


Figure 9. Pareto optimal solution set diagram.

Figure 9 presents the obtained Pareto optimal solution set, which comprises a total of 148 data groups. The most favorable point recommended by the software has been selected. In accordance with manufacturing precision and process requirements, the seven dimensional parameters derived from the optimization have been rounded to suitable values for practical application and then submitted to simulation software for analysis. The stress response along the Z -axis under unit excitation as well as the validation results

for the battery pack's fatigue life, the maximum impact stress in the +Z direction, and the maximum impact stress in the -Z direction are all depicted in Figure 10.

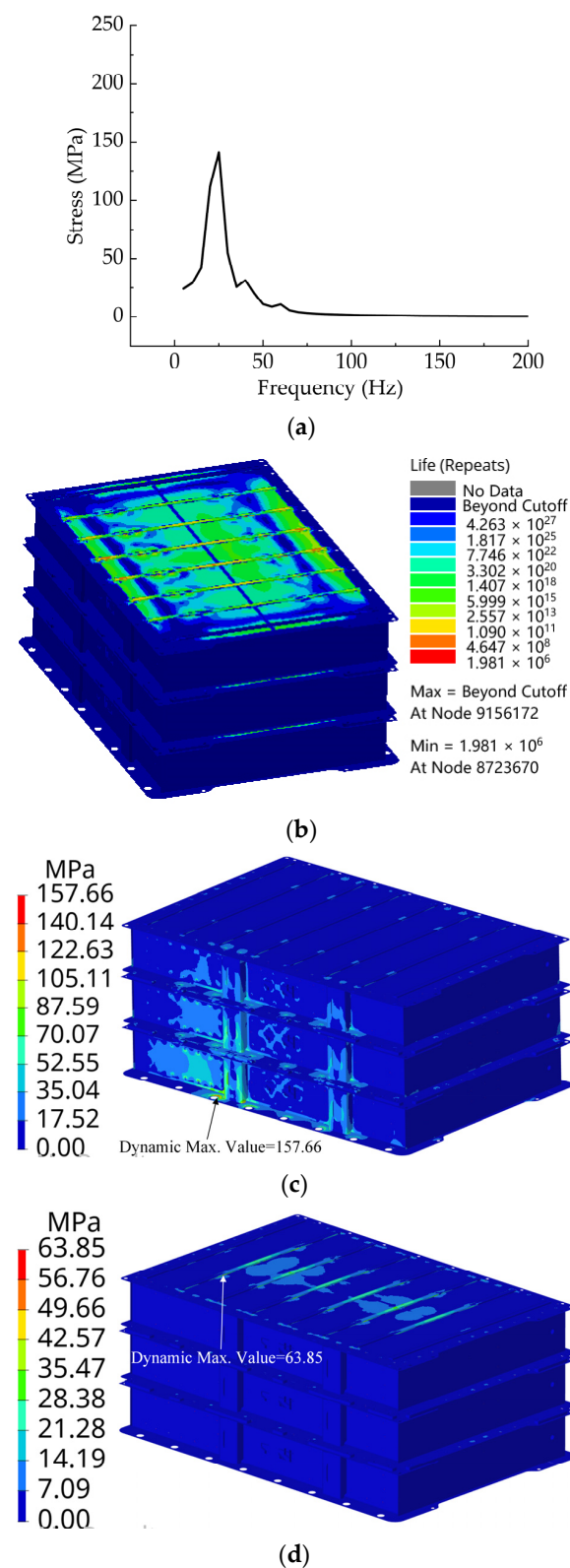


Figure 10. Structural responses after optimization: (a) Optimized frequency response diagram; (b) Optimized fatigue life contour map; (c) Post-optimization +Z mechanical impact maximum stress cloud diagram; (d) Post-optimization -Z mechanical impact maximum stress cloud diagram.

In Figure 10, based on the results of the optimized frequency response analysis, the Z-axis stress response curve of the battery pack under unit excitation is presented. The maximum response stress occurs at approximately 22 Hz, which corresponds to the first-order mode of the battery pack. Furthermore, after optimization, the maximum stress is reduced to 141.1 MPa, representing a decrease of 34.4% compared to before optimization, thereby enhancing fatigue life. Post-optimization, the lowest fatigue life of the battery pack is observed at the reinforcement ribs of the upper cover plate, with a minimum cycle count of 1,981,000 cycles. When applying +Z-direction mechanical impact to the optimized battery pack, it is noted that maximum stress occurs at the center mounting hole of the bottom installation plate and reaches 157.66 MPa. When −Z-direction mechanical impact is applied to this optimized structure, maximum stress appears at the position of cover plate reinforcement ribs and measures 63.85 MPa. A comparative analysis between structural responses before and after optimization for the battery pack is summarized in Table 3.

Table 3. Results of multi-objective optimization simulation validation.

Response Variable	Initial Value	Pareto Value	Simulation Value	Error/%
M/kg	987.80	922	931	0.98
L/cycle	746,200	2,018,334	1,981,000	1.85
Q/Hz	21.50	22.23	22.51	1.26
S ₁ /MPa	183.30	166.60	157.70	5.34
S ₂ /MPa	68.29	63.20	63.90	1.11

The results presented in Table 3 indicate that the relative errors between the simulated values of various responses and the Pareto optimal predictions obtained through multi-objective optimization do not exceed 10%. Specifically, the mass of the battery pack frame M, its fatigue life L, the first-order modal frequency Q, and the maximum stress under −Z direction impact are all controlled within a margin of error of 2%. This further demonstrates that the established Kriging surrogate model exhibits good accuracy and reliability. After optimization, the mass of the battery pack frame M was reduced by 56.8 kg, representing a decrease of 5.75% compared to its pre-optimization value. Additionally, the fatigue life L of the battery pack increased by 1,234,800 cycles, which corresponds to an enhancement factor of 1.65 times over its initial state. In terms of other structural response variables, the first-order modal frequency Q increased by 1.01 Hz; meanwhile, +Z direction maximum stress decreased by 25.6 MPa, and −Z direction maximum stress decreased by 4.39 MPa. Overall, it can be concluded that, after optimization, not only does the battery pack meet fundamental static and dynamic structural requirements but it also achieves a significant reduction in weight while substantially enhancing its fatigue life.

5. Conclusions

(1) In response to the issue of structural failure caused by impact loads and random vibration loads on specialized battery packs for electric engineering machinery, a finite element model of the battery pack was established. The battery pack underwent constrained modal analysis, mechanical shock simulation, and fatigue life assessment to identify the response variables for multi-objective optimization.

(2) Utilizing a comprehensive contribution method, the thickness of components was selected as a design variable. From ten sets of parts, multiple design variables for multi-objective optimization were identified. The maximum stress under mechanical shock conditions and the first-order modal frequency were set as constraint conditions, while

minimizing mass and maximizing fatigue life were defined as objectives in the dimensional optimization design.

(3) A Box–Behnken experimental design method was employed to conduct grouped experiments, and a high-precision Kriging approximation model was established. By integrating the NSGA-II optimization algorithm, 148 sets of Pareto non-dominated solutions were obtained, from which the optimal Pareto solution for multi-objective optimization was derived.

(4) The optimized frame of the electric engineering machinery-specific battery pack exhibited a weight reduction of 56.8 kg, resulting in a total weight of 931 kg, which represents a decrease of 5.75% compared to its pre-optimization state. Furthermore, the fatigue life of the optimized battery pack increased by 1,234,800 cycles, demonstrating an enhancement factor of 1.65 times relative to its previous fatigue life, thus indicating significant performance improvement.

Author Contributions: Conceptualization, Z.L. and F.W.; methodology, Z.L. and F.W.; software, Z.L. and J.Q.; validation, Z.L., M.Z. and F.W.; formal analysis, Z.L., J.Q. and F.W.; investigation, J.Q., M.Z. and M.X.; resources, M.Z. and F.W.; data curation, Z.L., F.W. and M.X.; writing—original draft preparation, Z.L. and J.Q.; writing—review and editing, Z.L., J.Q., M.X., W.H. and F.W.; visualization, Z.L., J.Q. and F.W.; supervision, M.Z. and W.H.; project administration, M.Z. and W.H.; funding acquisition, W.H. All authors have read and agreed to the published version of the manuscript.

Funding: This research was funded by the Guangxi Science and Technology Major Program (AA23062072 and AA24206034).

Data Availability Statement: Data are contained within the article.

Acknowledgments: Thanks to Wei Huang’s guidance and the help of the research team members. Without their guidance and help, the study could not be completed.

Conflicts of Interest: Author Mr. Ming Zhao and Mr. Fangming Wu was employed by the company Guangxi Liugong Machinery Co., Ltd. The remaining authors declare that the research was conducted in the absence of any commercial or financial relationships that could be construed as a potential conflict of interest. The authors declare that this study received funding from Guangxi Liugong Machinery Co., Ltd. The funder had the following involvement with the study: Multi-Objective Structural Optimization Design for Electric Excavator-Specific Battery Packs with Impact Resistance and Fatigue Endurance. The authors declare that this study received funding from Guangxi Liugong Machinery Co., Ltd. The funder was not involved in the study design, collection, analysis, interpretation of data, the writing of this article or the decision to submit it for publication.

References

1. Tong, Z.; Miao, J.; Li, Y.; Tong, S.; Zhang, Q. Development of electric construction machinery in China: A review of key technologies and future directions. *J. Zhejiang Univ. Sci. A* **2021**, *22*, 245–264. [[CrossRef](#)]
2. Huang, X.; Huang, Q.; Cao, H.; Cao, H. Battery capacity selection for electric construction machinery considering variable operating conditions and multiple interest claims. *Energy* **2023**, *275*, 127454. [[CrossRef](#)]
3. Lin, T.; Wang, L.; Huang, W.; Ren, H. Performance analysis of an automatic idle speed control system with a hydraulic accumulator for pure electric construction machinery. *Autom. Constr.* **2017**, *84*, 184–194. [[CrossRef](#)]
4. Huang, X.; Yan, W.; Cao, H.; Chen, S. Prospects for purely electric construction machinery: Mechanical components, control strategies and typical machines. *Autom. Constr.* **2024**, *164*, 105477. [[CrossRef](#)]
5. Daniele, B.; Iora, P.; Tribioli, L.; Uberti, S. Electrification of Compact Off-Highway Vehicles-Overview of the Current State of the Art and Trends. *Energies* **2021**, *14*, 5565. [[CrossRef](#)]
6. Lin, T.; Lin, Y.; Ren, H.; Chen, H.; Chen, Q.; Li, Z. Development and key technologies of pure electric construction machinery. *Renew. Sustain. Energy Rev.* **2020**, *132*, 110080. [[CrossRef](#)]
7. Li, L.; Zhang, T.; Wu, K.; Lu, L.; Lin, L.; Xu, H. Design and Research on Electro-Hydraulic Drive and Energy Recovery System of the Electric Excavator Boom. *Energies* **2022**, *15*, 4757. [[CrossRef](#)]

8. Ge, L.; Quan, L.; Zhang, X.; Zhao, B.; Yang, J. Efficiency improvement and evaluation of electric hydraulic excavator with speed and displacement variable pump. *Energy Convers. Manag.* **2017**, *150*, 62–71. [[CrossRef](#)]
9. Kaliaperumal, M.; Dharanendrakumar, M.S.; Prasanna, S.; Abhishek, K.V.; Chidambaram, R.K.; Adams, S.; Zaghib, K.; Reddy, M.V. Cause and Mitigation of Lithium-Ion Battery Failure—A Review. *Materials* **2021**, *14*, 5676. [[CrossRef](#)] [[PubMed](#)]
10. Arora, S.; Shen, W.; Kapoor, A. Review of mechanical design and strategic placement technique of a robust battery pack for electric vehicles. *Renew. Sustain. Energy Rev.* **2016**, *60*, 1319–1331. [[CrossRef](#)]
11. Hendricks, C.; Williard, N.; Mathew, S.; Pecht, M. A failure modes, mechanisms, and effects analysis (FMMEA) of lithium-ion batteries. *J. Power Sources* **2015**, *297*, 113–120. [[CrossRef](#)]
12. Kin, H.; Kim, G.; Ji, W.; Lee, Y.; Jang, S.; Shin, C. Random vibration fatigue analysis of a multi-material battery pack structure for an electric vehicle. *Funct. Compos. Struct.* **2021**, *3*, 025006.
13. Shui, L.; Chen, F.; Garg, A.; Peng, X.; Bao, N.; Zhang, J. Design optimization of battery pack enclosure for electric vehicle. *Struct. Multidiscip. Optim.* **2018**, *58*, 331–347. [[CrossRef](#)]
14. Pan, Y.; Xiong, Y.; Dai, W.; Diao, K.; Wu, L.; Wang, J. Crush and crash analysis of an automotive battery-pack enclosure for lightweight design. *Int. J. Crashworthiness* **2022**, *27*, 500–509. [[CrossRef](#)]
15. Zhang, X.; Yue, X.; Pan, Y.; Du, H.; Liu, B. Crushing stress and vibration fatigue-life optimization of a battery-pack system. *Struct. Multidiscip. Optim.* **2023**, *66*, 48. [[CrossRef](#)]
16. Pan, Y.; Xiong, Y.; Wu, L.; Diao, K.; Guo, W. Lightweight Design of an Automotive Battery-Pack Enclosure via Advanced High-Strength Steels and Size Optimization. *Int. J. Automot. Technol.* **2021**, *22*, 1279–1290. [[CrossRef](#)]
17. Zhang, X.; Xiong, Y.; Pan, Y.; Xu, D.; Kawsar, I.; Liu, B.; Hou, L. Deep-learning-based inverse structural design of a battery-pack system. *Reliab. Eng. Syst. Saf.* **2023**, *238*, 109464. [[CrossRef](#)]
18. Yang, R.; Zhang, W.; Li, S.; Xu, M.; Huang, W.; Qing, Z. Finite Element Analysis and Optimization of Hydrogen Fuel Cell City Bus Body Frame Structure. *Appl. Sci.* **2023**, *13*, 10964. [[CrossRef](#)]
19. Yu, S.; Zhang, Y.; Liu, X. Vibration Analysis and Control of the Hydraulic Excavator's Power System. *Noise Vib. Control* **2017**, *37*, 203–206.
20. GB/T 44257.1-2024; Traction Battery of Electric Earth-Moving Machinery-Part 1: Safety Requirements. The National Standardization Administration of China: Beijing, China, 2024.
21. Dai, J.; Xiong, F.; Liu, J.; Chen, C.; Chen, H.; Yang, Y. Random vibration fatigue analysis and structural design improvement of battery pack based on an vehicle. *J. Mech. Strength* **2020**, *42*, 1266–1270.
22. Li, J.; Hu, G.; Chen, J. Analysis and Optimization of Fatigue Caused by Vibrations in the Quick-Replacement Battery Box for Electric Vehicles. *World Electr. Veh. J.* **2023**, *14*, 226. [[CrossRef](#)]
23. Debnath, D.; Ray, S.; Chakraborty, K. Development of a statistical model for reliability analysis of hybrid off-grid power system (HOPS). *Energy Strategy Rev.* **2016**, *13–14*, 213–221. [[CrossRef](#)]
24. Li, M.; He, X.; Zhu, G.; Liu, J.; Gou, K.; Wang, X. Modeling and Parameter Calibration of Morchella Seed Based on Discrete Element Method. *Appl. Sci.* **2024**, *14*, 11134. [[CrossRef](#)]
25. Gao, F.; Wang, H.; Li, Y.; Zio, E. Distributed-collaborative surrogate modeling approach for creep-fatigue reliability assessment of turbine blades considering multi-source uncertainty. *Reliab. Eng. Syst. Saf.* **2024**, *250*, 110316. [[CrossRef](#)]
26. Kwon, H.; Choi, S. A trended Kriging model with R 2 indicator and application to design optimization. *Aerosp. Sci. Technol.* **2015**, *43*, 111–125. [[CrossRef](#)]
27. Deb, K.; Agrawal, S.; Pratap, A.; Meyarivan, T. A fast and elitist multiobjective genetic algorithm: NSGA-II. *IEEE Trans. Evol. Comput.* **2002**, *6*, 182–197. [[CrossRef](#)]
28. Xiong, Y.; Pan, Y.; Wu, L.; Liu, B. Effective weight-reduction- and crashworthiness-analysis of a vehicle's battery-pack system via orthogonal experimental design and response surface methodology. *Eng. Fail. Anal.* **2021**, *128*, 105635. [[CrossRef](#)]

Disclaimer/Publisher's Note: The statements, opinions and data contained in all publications are solely those of the individual author(s) and contributor(s) and not of MDPI and/or the editor(s). MDPI and/or the editor(s) disclaim responsibility for any injury to people or property resulting from any ideas, methods, instructions or products referred to in the content.